INTERFACE SCIENCE 3, 289–302 (1996)

First-Principles Study of the α-Al_2O_3(0001)/Cu(111) Interface

G.L. ZHAO
Department of Materials and Engineering, University of Michigan, Ann Arbor, MI 48109-2136

J.R. SMITH
Physics and Physical Chemistry Department, GM R&D Center, Warren, MI 48090-9055

J. RAYNOLDS AND D.J. SROLOVITZ
Department of Materials and Engineering, University of Michigan, Ann Arbor, MI 48109-2136

Received May 27, 1995; Revised February 16, 1996

Abstract. Adhesive energetics and interfacial electronic structures have been computed from first principles for the Cu/Al_2O_3 interface. Recent transmission electron microscopy results of Cu grown by molecular beam epitaxy on Al_2O_3(0001) were helpful in modelling the interfacial atomic structure. We found that Al_2O_3(0001) relaxation effects can lower the work of adhesion W_{ad} by over a factor of 3. Our computed W_{ad} value is in reasonably good agreement with experiment, being somewhat larger, as expected from our assumption of a coherent interface. One might begin to understand this metal/ceramic adhesion as a competition between Cu and Al for oxide formation, which is easily won by Al. However this simple picture is complicated by several indications of a significant metallic/covalent component to the Cu/Al_2O_3 adhesive bond.

Keywords: adhesion, metal/ceramic bonding, quantum mechanical computations

1. Introduction

Alumina/metal interfaces are of significance in several industrial applications, including metal-matrix composites [1], electronic packaging [2], and exhaust-gas catalysis [3]. Copper is commercially joined to alumina for electronic packaging and metallization applications [4]. Adhesion of metals to alumina is of importance in all these applications, particularly for the mechanical properties of metal-matrix composites [1].

Despite the technological importance, the fundamental theoretical understanding of ceramic/metal interfaces is in its infancy. There is very little known about ceramic/metal bond strengths or atomic arrangements at the interface. Because of the variety of elements and bond types (metallic, covalent, and ionic) in the ceramic/metal interface, the only way of obtaining reliable, accurate predictions of the structure and energetics in these systems is via first-principles computations. Recently, such first-principles calculations have been appearing in the literature. Schönberger et al. [5], have treated Ti and Ag on MgO. Hong et al. [6], carried out fully self-consistent, all-electron density-functional calculations for MgO/Ag and MgO/Al interfaces with and without interfacial monolayers of impurities. This first treatment of impurity effects on metal/ceramic adhesion revealed that impurities can change adhesive energies by over a factor of 2. Kruse et al. [7], have recently treated the Nb/Al_2O_3 interface.

The Cu/Al_2O_3 interface [8] is a good route to probe the fundamentals of metal/ceramic adhesion because atomically sharp interfaces have been produced by internal oxidation, solid state bonding, and vapor deposition [9]. Dehm et al. [9], prepared an epitaxial Cu film

on (0001)-oriented single crystal sapphire wafers by molecular beam epitaxy (MBE). They then performed TEM on these contamination free, epitaxial interfaces. Their TEM observations on this clean, epitaxial interface give us some knowledge about how to build the interface on the atomic level. Their transmission electron microscopy (TEM) on these interfaces showed a preferred (111) Cu on (0001) sapphire orientational relationship. While they found the interface to be epitaxial, they also found it to be incoherent. We are limited in the number of atoms per unit cell that we can treat in the rigorous, first-principles methods we employ. We therefore assume coherency and expect our work of adhesion W_{ad} between Cu and Al_2O_3 to be somewhat larger than experimental values taken from clean interfaces, as discussed further in the last paragraph of Section 3. Here W_{ad} is the binding energy between the two surfaces per cross-sectional area [6].

Interestingly enough, W_{ad} for metal-ceramic interfaces seemed to be well understood in 1965. McDonald and Eberhart [10] plotted experimental W_{ad} values for metals on Al_2O_3 versus free energies of oxide formation of these same metals and the results fell close to a straight line. However, when Chatain et al. [11], added a number of metals to the plot, the new data was not at all close to the line. This suggests the metal/ceramic interaction is more complicated than had been thought. In the following, we hope to make a contribution to the understanding of this interaction.

2. Calculational Method

The calculations were performed via a self-consistent first-principles LCAO (linear combination of atomic orbitals) method [12–14]. This method has been extensively used to study the electronic structure, optical properties, and lattice dynamics in many materials. In this method, the electronic eigenstates, $\Psi_{\vec{k}_\parallel n}(\vec{r})$, of the system associated with a Hamiltonian H, are expanded as a linear combination of Bloch-wave basis functions $\phi_{\alpha m}(\vec{k}_\parallel, \vec{r})$:

$$\Psi_{\vec{k}_\parallel n}(\vec{r}) = \sum_{\alpha m} C_{\alpha m}(\vec{k}_\parallel n)\phi_{\alpha m}(\vec{k}_\parallel, \vec{r}). \quad (1)$$

Here the Bloch wave functions are expressed as:

$$\phi_{\alpha m}(\vec{k}_\parallel, \vec{r}) = \frac{1}{\sqrt{N}} \sum_l e^{i\vec{k}_\parallel \cdot \vec{R}_l} u_{\alpha m}(\vec{r} - \vec{\tau}_m - \vec{R}_l), \quad (2)$$

where $\vec{k}_\parallel$ is a wave vector parallel to the interface; $u_{\alpha m}$ is the atomic wave function for the αth state of mth atom at the position of $\vec{\tau}_m$.

The coefficients $C_{\alpha m}$ are calculated from the secular equation

$$HC = \epsilon_n SC, \quad (3)$$

where H and S are the Hamiltonian and overlap matrices:

$$H_{\alpha m,\alpha' m'} = \int \phi^*_{\alpha m} H \phi_{\alpha' m'} d\vec{r} \quad (4)$$

and

$$S_{\alpha m,\alpha' m'} = \int \phi^*_{\alpha m} \phi_{\alpha' m'} d\vec{r}. \quad (5)$$

The Hamiltonian H is approximated by treating the exchange-correlation potential in the local density approximation.

The electron density ρ is calculated from the eigenfunctions of Eq. (3):

$$\rho(\vec{r}) = \sum_{\text{occ}} |\Psi_{\vec{k}n}(\vec{r})|^2. \quad (6)$$

where the summation extends over all of the occupied electronic states. The electron density $\rho(\vec{r})$ is then expanded in an auxiliary basis of Gaussian functions. This representation amounts to the approximation

$$\rho(\vec{r}) \approx \bar{\rho}(\vec{r}) = \sum_{mi} \rho_{mi} \sum_l e^{-\alpha_{mi}(\vec{r} - \vec{\tau}_m - \vec{R}_l)^2}, \quad (7)$$

where $\{\alpha_{mi}\}$ is a set of Gaussian exponentials which was optimized to give a best electron density fit to the results of first-principles calculation. Similarly, the exchange-correlation potential V_{xc} is expanded by the same set of Gaussian functions in the form

$$V_{xc} = \sum_{mi} X_{mi} \sum_l e^{-\alpha_{mi}(\vec{r} - \vec{\tau}_m - \vec{R}_l)^2}. \quad (8)$$

These Eqs. (3)–(8) are solved in a self-consistent procedure.

3. Results

3.1. Bulk α-Al_2O_3

The bulk electronic structure of α-Al_2O_3 was calculated and compared with a previous study as a preliminary test of the calculation method. The crystal

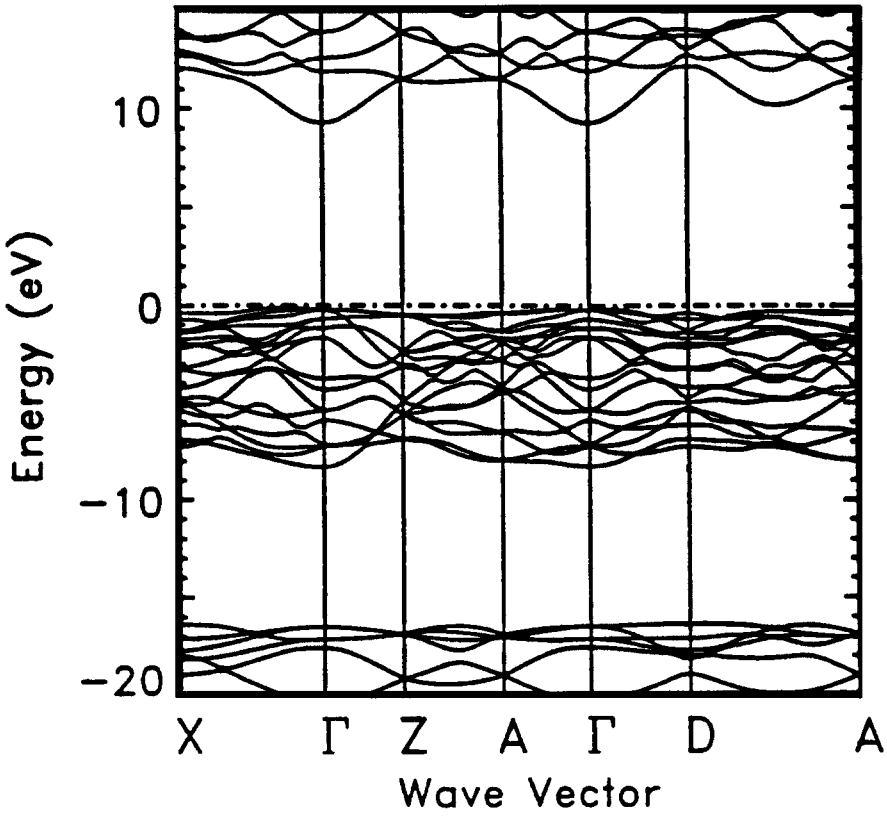

Figure 1. Electronic band structure of α-Al_2O_3 calculated from our self-consistent first-principles LCAO method. The dotted line indicates the top of the valence bands.

structure of α-Al_2O_3 is a corundum type having a trigonal space group D_{3d}^6 with two molecular formulas per unit cell. The lattice parameters of the rhombohedral unit cell are $a = 5.128$ Å, and $\alpha = 55.333°$. The aluminum atoms are at (4c) positions with u(Al) = 0.352; and oxygen atoms at (6e) position with u(O) = 0.556 in the notation of standard crystallographic tables. In the bulk calculation of the electronic structure, the Al atomic wave functions of 1s, 2s, and 2p were treated as core states, and 3s and 3p as valence states. Similarly, the 1s oxygen orbital was treated as a core orbital, and 2s and 2p as valence states. The atomic wave functions were carefully constructed from a self-consistent solution of the Schrödinger equation in which the atomic wave functions were expanded as a linear combination of Gaussian orbitals. The contracted atomic wave functions were used in the study of the bulk electronic structure. In the self-consistent calculation of the bulk electronic structure, 19 k-points in the irreducible Brillouin zone were used with proper weight for different k-points. In the self-consistent calculation, the valence electron density fit error was about 0.013 out of 48 total electrons. The fit was subsequently renormalized to give the exact total number of valence electrons. The calculated band structure is given in Fig. 1. The electronic band structure of α-Al_2O_3 in Fig. 1 is very similar to that reported in previous studies (see, e.g., Fig. 2 of [12]). The calculated band gap is about 9 eV and is in a good agreement with experimental results of 9.0 to 9.5 eV. This good agreement may be fortuitous, however, since density functional theory does not typically yield accurate predictions of energy band gaps in semiconductors and insulators.

3.2. *α-Al_2O_3(0001) Surface and Cu(111) Surface*

In the adhesive process we will consider, we start with free surfaces and then compute the energy changes as we bring those surfaces into contact. First we will do computations for the corresponding free surfaces. We remarked earlier that it has been shown experimentally [9] that the preferred Cu/Al_2O_3 interface has a (111) Cu on a (0001) Al_2O_3 orientational relationship.

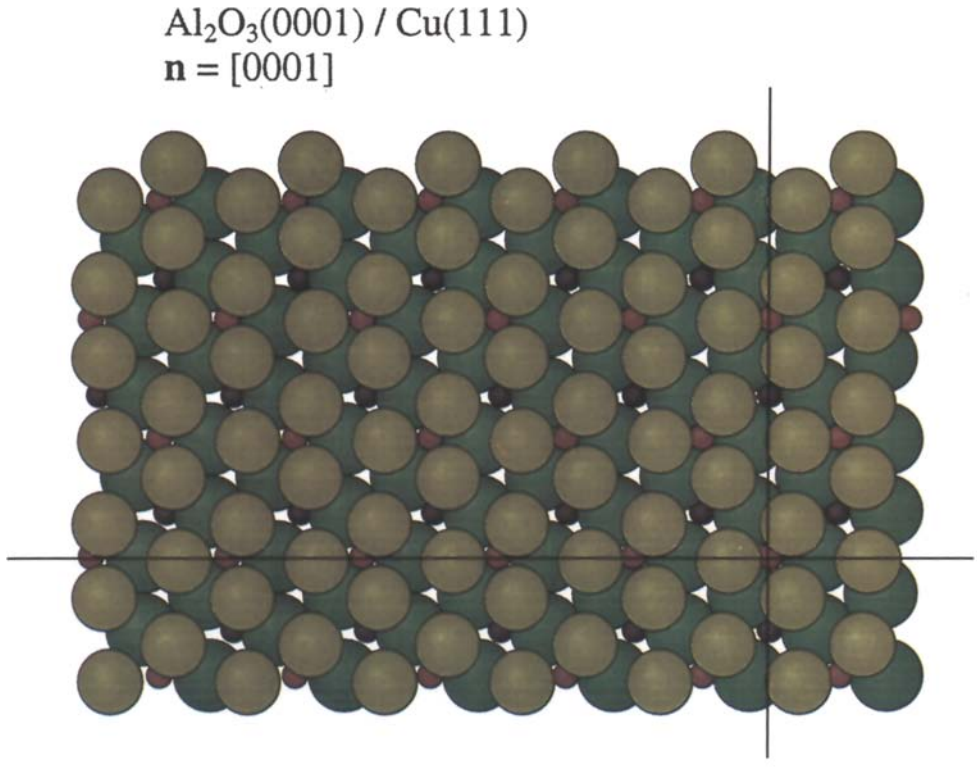

Figure 2. Ball model of the $Al_2O_3(0001)/Cu(111)$ interface. The yellow spheres are the Cu atoms, the small red spheres are the Al ions on the $Al_2O_3(0001)$ termination plane (i.e., closest to the Cu), the small dark spheres are the Al ions just below the O layer, and the green spheres are the O ions.

Let us first consider $Al_2O_3(0001)$. The aluminum and oxygen atoms form layers parallel to the (0001) surface of α-Al_2O_3. There are six formula units of Al_2O_3 in the bulk hexagonal cell of α-Al_2O_3 (see, e.g., Fig. 1 of [15]). The oxygen atoms form six layers in 18 (e) positions. The Al atoms are in 12 (c) positions forming 12 layers separated by oxygen layers. The atomic geometries chosen to represent the $Cu(111)/Al_2O_3(0001)$ are shown in Figs. 2–4. The smaller red spheres in these figures are the Al ions, the green spheres are the O ions, and the yellow spheres are the Cu atoms. Note that the $Al_2O_3(0001)$ surface is Al terminated. It has been shown [16] that the $Al_2O_3(0001)$ cleavage energy for oxygen termination is almost twice as large as for aluminum termination. Experimentally [17] both (1×1) and reconstructed surfaces have been observed. Since it has been found that Cu(111) is epitaxial with $Al_2O_3(0001)$, we will focus on the (1×1) surface of Al_2O_3. Periodic boundary conditions were used to construct a unit cell for the self-consistent, first-principles calculation of the $Al_2O_3(0001)$ surface. The unit cell used in this surface calculation is half of the bulk hexagonal supercell. Fifteen atoms (6 aluminum and 9 oxygen atoms) were used in the calculation. Along the c-axis, there are three oxygen layers and 6 aluminum layers. There are three oxygen atoms on an oxygen layer and one aluminum atom per aluminum layer in the hexagonal unit cell.

Table 1 compares our predicted surface energy for the unrelaxed $Al_2O_3(0001)$ surface with the predictions of two other groups [16, 18]. One can see that all three predictions are in close agreement.

It has been found [18] that the surface energy of $Al_2O_3(0001)$ can be significantly lowered via

Table 1. Surface energy of α-$Al_2O_3(0001)$ in J/m^2.

Unrelaxed surface:	
Reported results	3.7[a]
	3.77[b]
Present work	3.68
Relaxed surface:	
Reported result	1.76[b]

[a]Ref. 16, [b]Ref. 18.

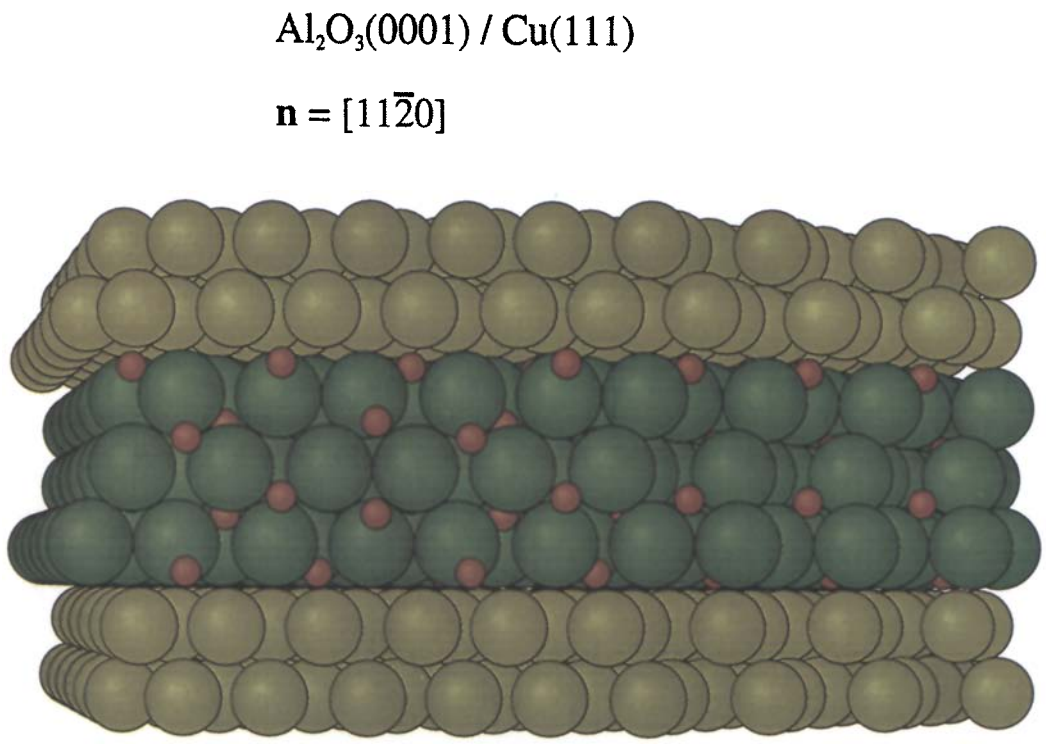

Figure 3. Ball model of Al_2O_3(0001)/Cu(111) interface. This shows the equilibrium separation between the Cu and Al_2O_3. The direction of view is [11$\bar{2}$0]. The planar spacing within the Al_2O_3(0001) is the bulk (unrelaxed) spacing.

substantial planar relaxations. The largest relaxation occurs between the surface Al layer and the O layer beneath it, with the Al-O interplanar spacing decreased [18] by 86%. That relaxation, and lesser ones deeper into the bulk were reported to lower the surface energy by 2.01 J/m^2, as is shown in Table 1.

The Cu(111) surface was also examined in this study and compared with a previous first-principles calculation [13]. The copper atomic states of 1s, 2s, 3s, 2p and 3p were treated as core states, and these together with 4s, 3d and 4p functions completed the basis set. The calculations were performed on three and five Cu(111) layer slabs respectively. The quality of the calculation can be first checked by the error in the electron density fit. The total number of electrons determined from integrating the electron density fit was within 0.026 percent of the exact number. Comparison of the calculated work function with experimental results is also an indication of the error since the work function is quite sensitive to charge polarization at the surface. The calculated work function, which is defined as the Fermi energy, is about 5.3 eV from this calculation. The experimental result is [19] 4.94 eV and the previous calculation [13] gave a value at about 5.1 eV. The calculated surface energy of Cu (111) is listed in Table 2 and one can see that it agrees well with the earlier studies.

Table 2. Surface energy of Cu(111) in J/m^2.

Unrelaxed surface:	
Reported results	2.1[a]
	2.016[b]
Present work	2.07

[a]Ref. 13; [b]Ref. 29.

3.3. *α-Al_2O_3 (0001)/Cu (111) Interface*

While in principle we could determine the Cu/Al_2O_3 interfacial atomic structure by minimizing the total energy, in practice that would require a considerable amount of computational time. Thus it is very helpful to have the TEM results [9] for Cu grown by MBE on Al_2O_3(0001). As noted in the Introduction, the authors of [9] found that growth occurs with the Cu(111) planes parallel to Al_2O_3(0001) at 200°C. The experiment doesn't tell us whether the Al_2O_3(0001)

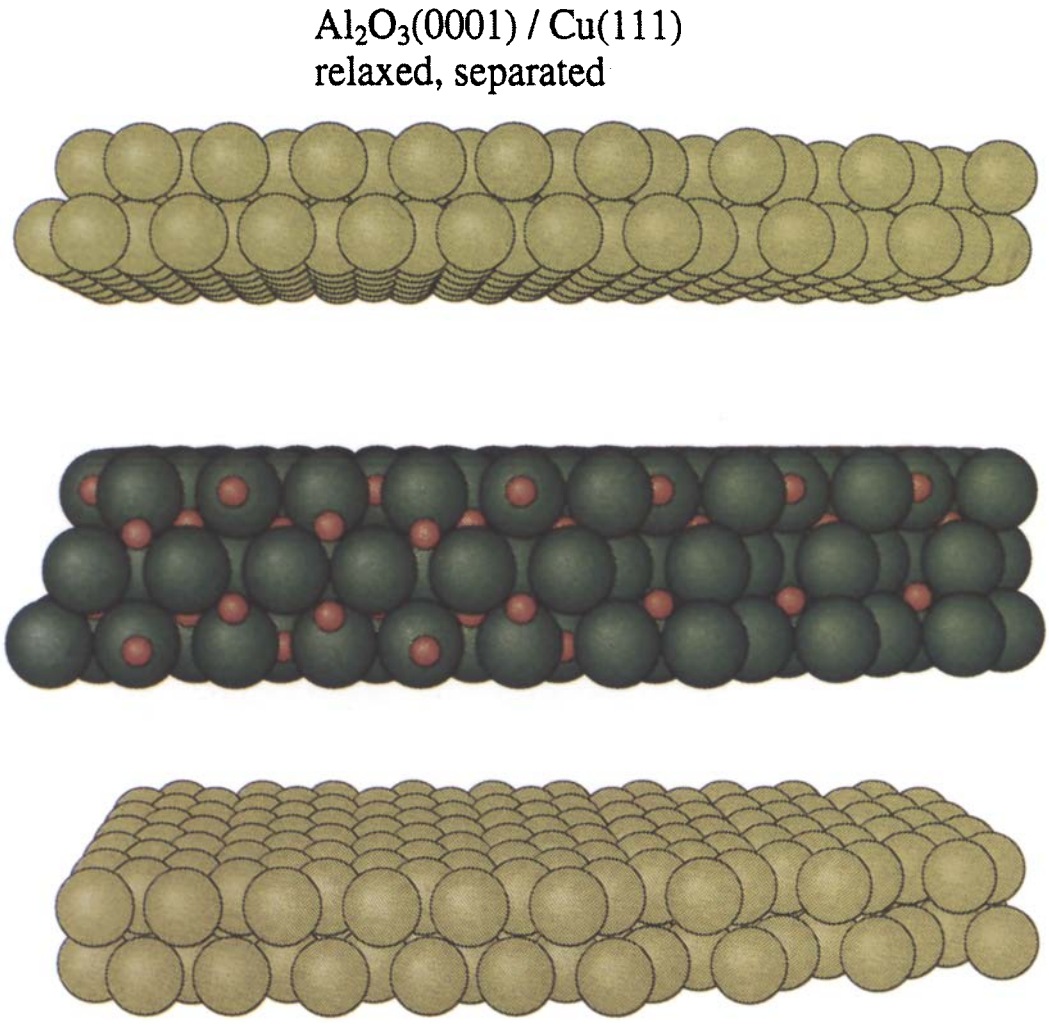

Figure 4. Ball model of the $Al_2O_3(0001)$/Cu(111) interface. This shows the large-separation configuration, with the $Al_2O_3(0001)$ relaxed. Again the direction of view is $[11\bar{2}0]$.

is O or Al terminated. As noted earlier, at large Cu(111) to $Al_2O_3(0001)$ separations we would expect the $Al_2O_3(0001)$ to be Al terminated since it has been found [16] that the Al-terminated $Al_2O_3(0001)$ surface energy is almost a factor of 2 smaller than the O-terminated value. At smaller Cu(111) to $Al_2O_3(0001)$ separations one would also expect the $Al_2O_3(0001)$ to be Al-terminated because, as can be seen from Fig. 3 of [11], the Al oxide formation energy is an order of magnitude larger than that for Cu. Thus we would not expect Cu to displace Al in the interfacial oxide bonding.

In Figs. 2–4, we have shown an atomic configuration consistent with these observations. In Fig. 2 only the Cu layer closest to the Al_2O_3 has been shown so that Al_2O_3 can be seen through the Cu. There are 3 different 3-fold oxygen sites for the Cu lattice to occupy. Two are over Al atoms: one over a surface Al atom and one over an Al atom just below the surface. In our earlier [6] metal/MgO studies, we found that the lowest energy configuration occurred for the metal atoms on top of the O atoms rather than on top of the Mg atoms. Based on that, we placed the Cu layer on the 3-fold oxygen site not containing an Al atom. This lessens the probability for steric hindrance between the Al and Cu, and allows the Cu to move in closer to the O atoms. This competition between the Al and Cu for the oxygen bond is key and will be discussed further below. The next Cu layer is placed in the 3-fold Cu site over the surface oxygen atoms. Because it is well known that metallic screening lengths are short, our experience (see, e.g., [20])

suggests that it is adequate to represent the Cu(111) film by a 2 Cu layer slab, as shown in Figs. 3 and 4.

The lattice mismatch between Al_2O_3(0001) and Cu(111) is 7%. In order to make the calculation tractable, we stretched the Cu(111) into commensuration with the Al_2O_3(0001). We decreased the spacing between the Cu(111) layers correspondingly to conserve the (bulk) Cu volume per atom. Experiments have shown [9] that this misfit is at least partially relieved by forming an incoherent interface. In these calculations, we have neglected the effects of this incoherency. Therefore, our analysis will underestimate the interface energy and overestimate the work of adhesion.

Finally, we return to the finding [18] for the free Al_2O_3(0001) surface of a relatively large planar relaxation. Clearly, at large Cu(111)/Al_2O_3(0001) spacings one would expect the Al_2O_3(0001) surface to relax. However, near the equilibrium spacing between Cu(111) and Al_2O_3(0001) the "dangling" Al_2O_3(0001) bonds would tend to be terminated on Cu atoms, and one might expect the Al_2O_3(0001) interplanar spacings to be closer to their bulk values. It is commonly found that overlayers tend to lessen or eliminate surface reconstructions. Thus we will first compute Cu(111)/Al_2O_3(0001) adhesive energy curves with the Al_2O_3(0001) having the bulk interplanar spacing, as shown in Fig. 3. Ultimately, however, the final or separated state will be allowed to relax, as shown in Fig. 4. We will see that this relaxation plays an important role in the work of adhesion W_{ad}.

Figure 5 is a total self-consistent electron density map on a plane perpendicular to the interface (shown

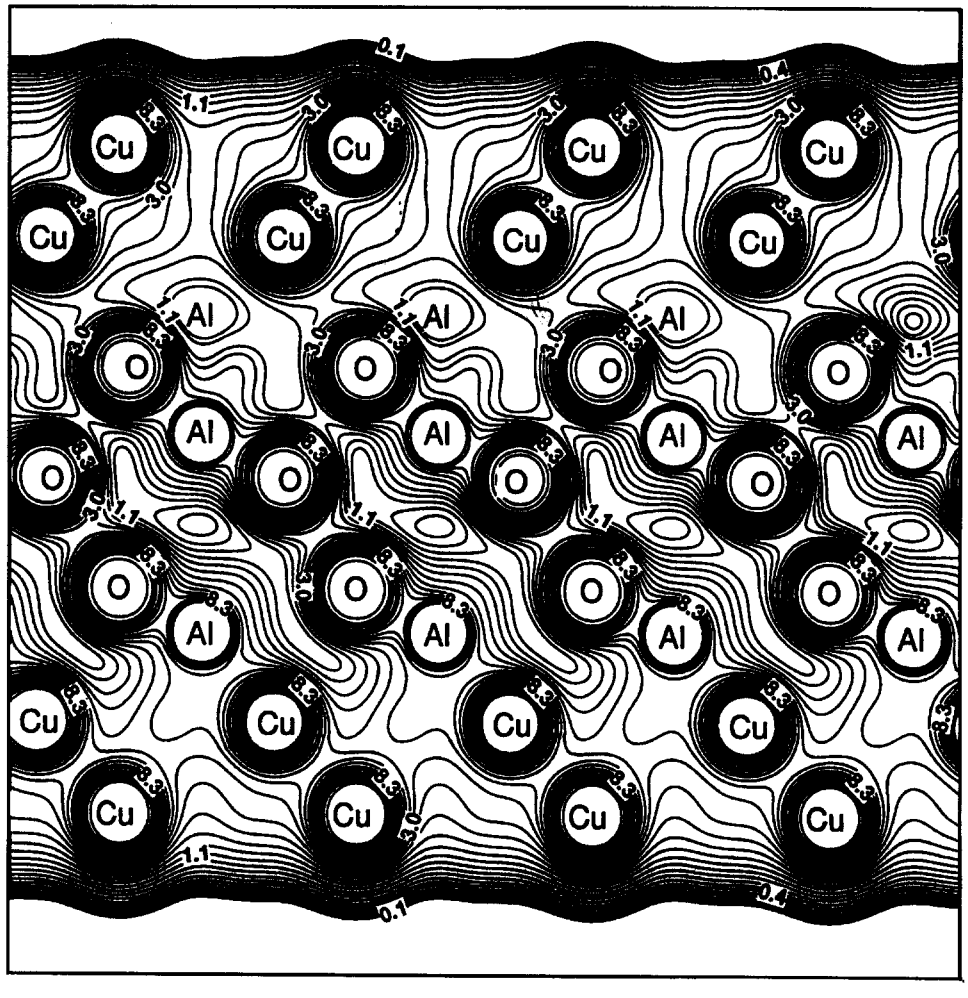

Figure 5. The total electron density map on a plane perpendicular to the Cu(111)/Al_2O_3(0001) interface cutting through the interface oxygen atoms along the horizontal line shown in Fig. 2.

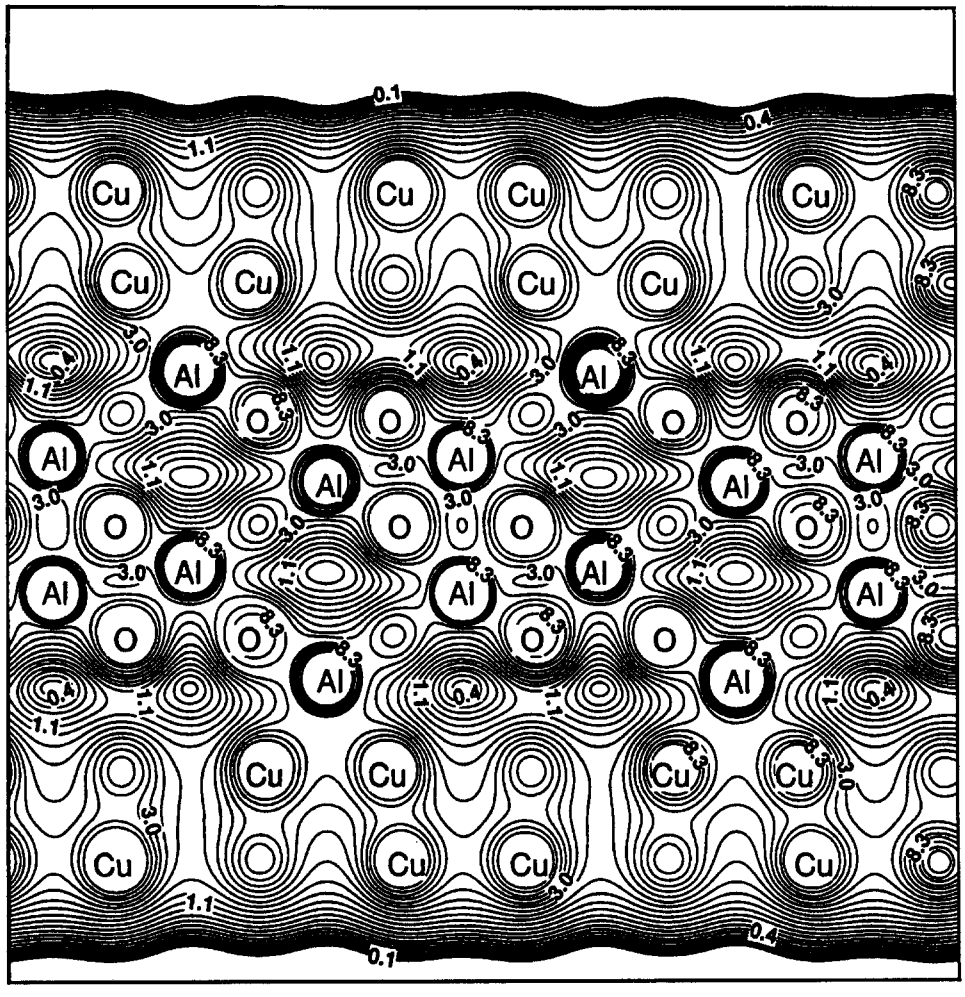

Figure 6. The total electron density map on a plane perpendicular to the interface cutting through the interface aluminum atoms along the vertical line shown in Fig. 2.

by the horizontal line in Fig. 2). This plane cuts through the oxygen atoms at the interface. There are two Cu(111) interfaces, one on either side of the Al_2O_3 slab (Fig. 5). The unit cell has no reflection symmetry in the direction perpendicular to the interface. The middle of the unit cell is α-Al_2O_3 with three oxygen planes and 6 aluminum layers. Because of the nature of the hexagonal structure, some of the aluminum planes can not be directly seen on this cut in Fig. 5. Between two oxygen planes, there are two aluminum atomic layers. The Al atoms follow the 3-fold site symmetry of the hexagonal structure and the two Al layers are shifted by a relatively small distance along the *c*-axis. The positions of the aluminum atoms can be seen from Fig. 6. Figure 6 shows the electron density on a second plane perpendicular to the interface, as shown by the vertical line in Fig. 2. The oxygen and copper atoms are not on this plane, but some of these atoms can still be identified from the electron density distribution as labeled in Fig. 6. There is some suggestion in both Figs. 5 and 6 of electron densities between atoms like one finds in covalent and in metallic bonding. The strong ionic component to the Al_2O_3 bonding is well known [22]. These contours suggest some covalent component to the Al_2O_3 bonding and the Cu—O bonding as well. There is little or no evidence of this between Cu and Al. This would suggest that both the Cu and Al are bonding primarily to the O atoms. Figures 7, 8, and 9 show the electron density maps on planes through the Cu, Al, and O atomic layers at the interface. The 3-fold sites of oxygen layers are fully occupied by O atoms. Similarly for the copper layers.

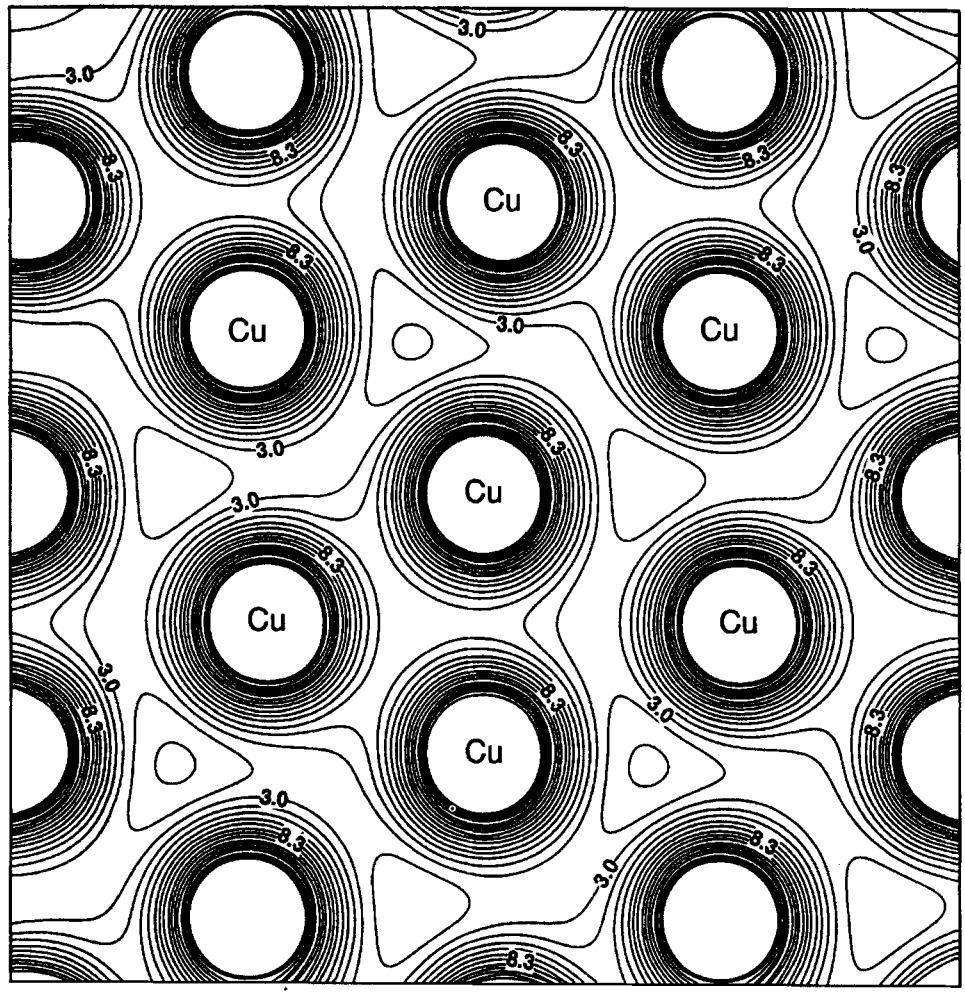

Figure 7. The total electron density map on a plane parallel to the interface cutting through the nuclei of the Cu layer at the interface.

But the aluminum atoms only take one of the 3-fold sites and strongly bond to oxygen atoms. For orientation, one should refer to Fig. 2. Evidence for both Cu—O and Al—O bonds can be found in the contours of Figs. 7, 8, and 9. The distance between the oxygen layer and aluminum layer along the c (or z) direction is 0.84 Å [18]. The distance between the aluminum and copper atomic layers was found to be 1.69 Å, as determined by the minimum in the energy versus separation curve, and is much larger than the Al—O plane separation. At equilibrium, there is then no steric hindrance between Cu atoms and Al ions. This larger separation is consistent with a weaker ionic character of the interfacial Cu—O bond as compared to the Al—O bond.

The work of adhesion, W_{ad}, of α-Al_2O_3(0001)/Cu(111) was calculated using the self-consistent first-principles LCAO method. In this self-consistent calculation, seven k-points in the two dimensional irreducible Brillouin zone with proper weights were used. W_{ad}, which is a difference in total energies between large and equilibrium spacings per unit cross-sectional area (as defined in the introduction), did not change significantly from the test case of four k-points calculation. This is an indication that seven k-points with proper weights in the self-consistent calculation should be adequate. The total valence electron density fit error was about 0.1% and was considered acceptable. The calculated adhesive energy curve is given in Fig. 10. Here d is the separation between the copper atomic layer and the aluminum layer at the interface. The adhesive energy results were also fitted to the universal-binding-energy relation (UBER) [23]. The symbols are the calculated data. The solid line is the fitted UBER. Note that the calculated points

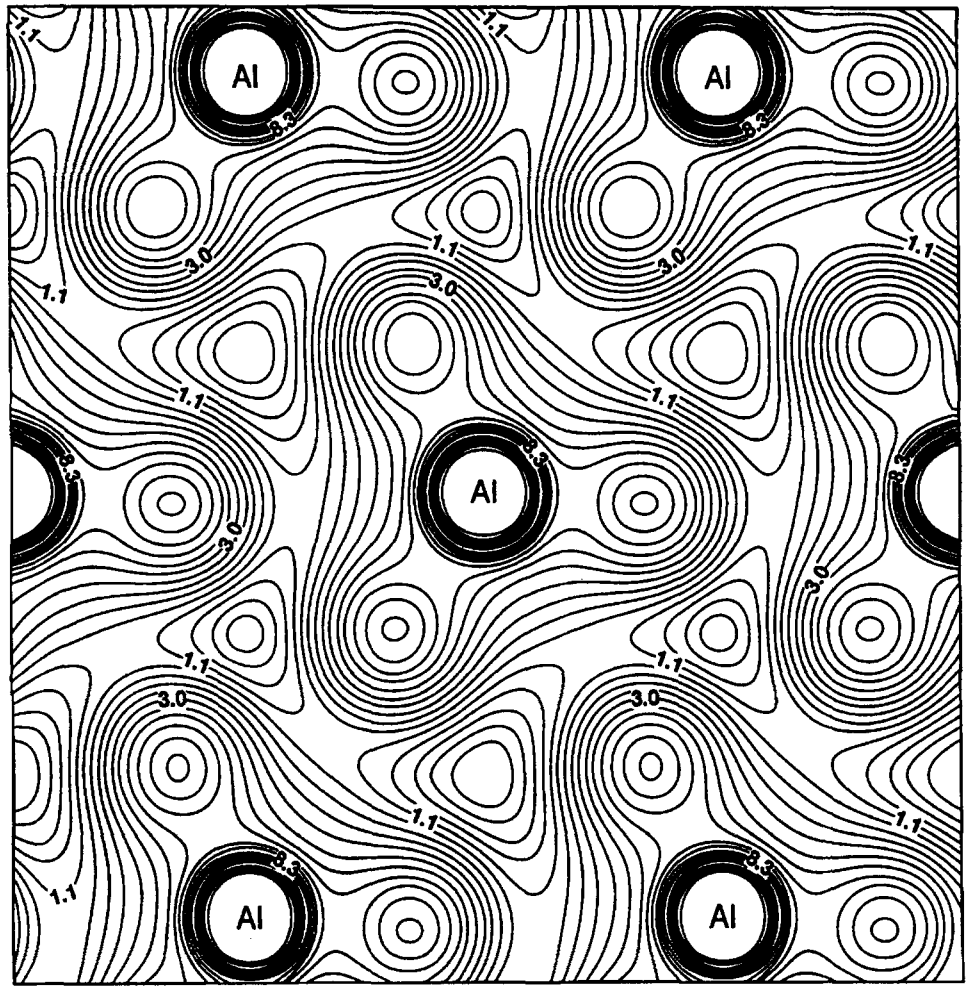

Figure 8. The total electron density map on a plane parallel to the interface cutting through the nuclei of the Al layer at the interface.

fall reasonably close to the universal binding energy relation. Since the UBER was first discovered [23] for bimetallic adhesion (and can be well represented by an exponential form), the agreement here suggests that there is a significant covalent/metallic component to the Cu/Al_2O_3 interfacial bond. The adhesive energy of the unrelaxed interface was determined to be 2.9 J/m^2 from the UBER curve in Fig. 10. Because of the scatter of the points about the UBER in Fig. 10, we estimate the uncertainty in W_{ad} to be ± 0.3 J/m^2.

In this calculation, when the Cu atoms were put on the surface of Al_2O_3 or pulled away, no relaxation of the atoms was included in the total energy calculation. Only the distance (d) between the Cu slab and the Al_2O_3 substrate was changed. We refer to this as an unrelaxed case. The unrelaxed W_{ad} of 2.9 J/m^2 is significantly larger than the 1.9 J/m^2 we [6] found earlier for Ag/MgO(100). This is perhaps to be expected, since the surface energy of unrelaxed $Al_2O_3(0001)$ is just over a factor of 2 larger than that of MgO(100) (1.8 J/m^2, see [5]), and the Cu(111) surface energy shown in Table 2 is larger than that of Ag(100) (1.5 J/m^2, see [6]).

As noted earlier, the $Al_2O_3(0001)$ free surface exhibits substantial planar relaxation, lowering [18] the surface energy by 2.01 J/m^2. Thus as $Cu(111)/Al_2O_3$ (0001) separations increase, one would expect the $Al_2O_3(0001)$ surface to approach the relaxed free surface configuration. This leads to a lowering of W_{ad} by 2.01 J/m^2 to 0.9 J/m^2. Thus the relaxation of the $Al_2O_3(0001)$ is a very important contributor to W_{ad}.

Finally, we compare our computed W_{ad} value of 0.9 J/m^2 with measured values. As our calculations are for

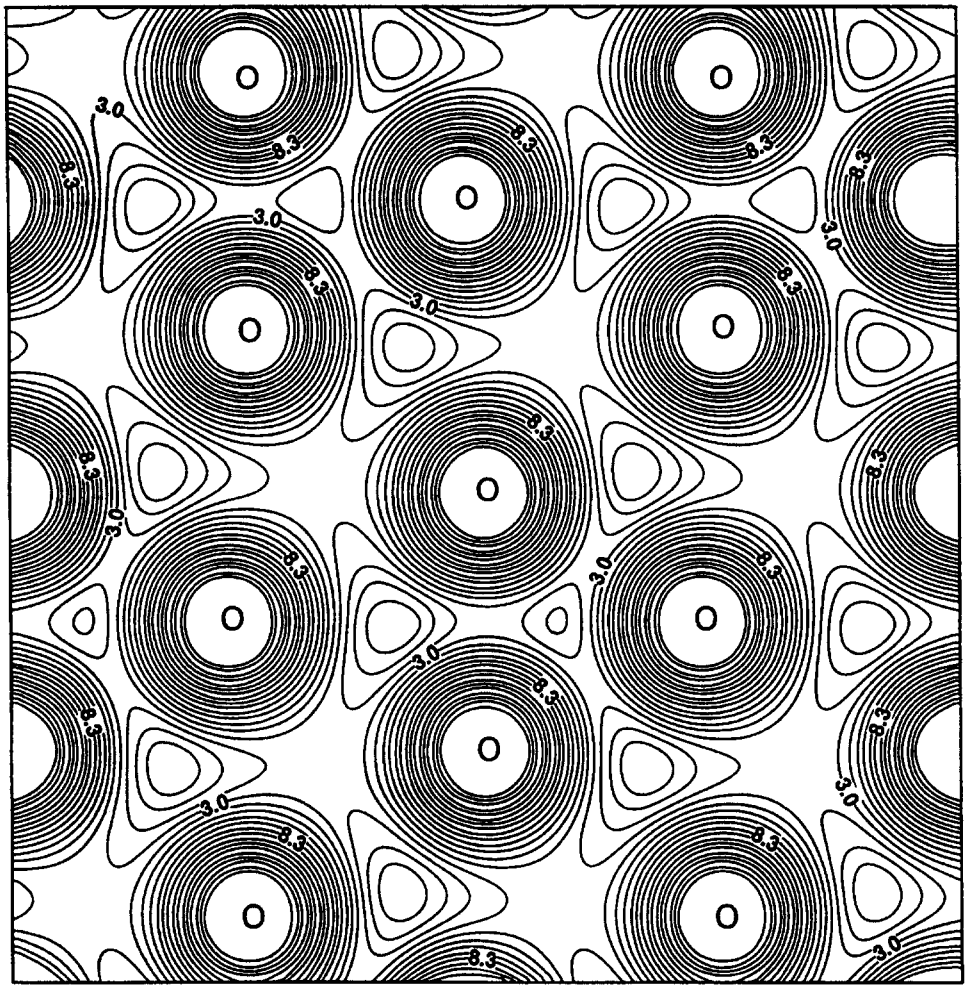

Figure 9. The total electron density map on a plane parallel to the interface cutting through the nuclei of the oxygen layer at the interface.

solid-solid interfaces, the measured values of Pilliar and Nutting [24] are most appropriate. The work of adhesion may be written as:

$$W_{ad} = (1 - \beta)\gamma_{Cu}, \tag{9}$$

where γ_{Cu} is the copper surface energy and $\beta = 0.66$ was determined by Pilliar and Nutting [24] based upon measurements of the shape of faceted Cu particles on sapphire. Taking our computed value of γ_{Cu} from Table 2 and $r_1/r_2 = 0.66$ as was reported in [24], we find $W_{ad} = 0.714$ J/m^2. The second experimental W_{ad} value [11] listed in Table 3 is 0.441 as measured for liquid Cu drops on Al_2O_3. This value is further from our calculated value, as one might expect since we treat a solid-solid interface and the experiment is for a solid-liquid interface.

Table 3. Work of adhesion for Cu/Al_2O_3 in J/m^2.

Present work	Experiment
2.9 (Unrelaxed)	
0.9 (Relaxed)	0.71,[a] 0.441[b]

[a]Ref. 24; [b]Ref. 11.

One should expect the computed W_{ad} to be higher than the experimental W_{ad} for several reasons. First, it has been shown [6, 25] that W_{ad} is sensitive to impurity contamination at the interface. As neither experimental determination was done in ultra-high vacuum, one must expect contamination. We have found [6, 25] that typically—though not always—impurities lower W_{ad}. Secondly, as noted earlier, experiments

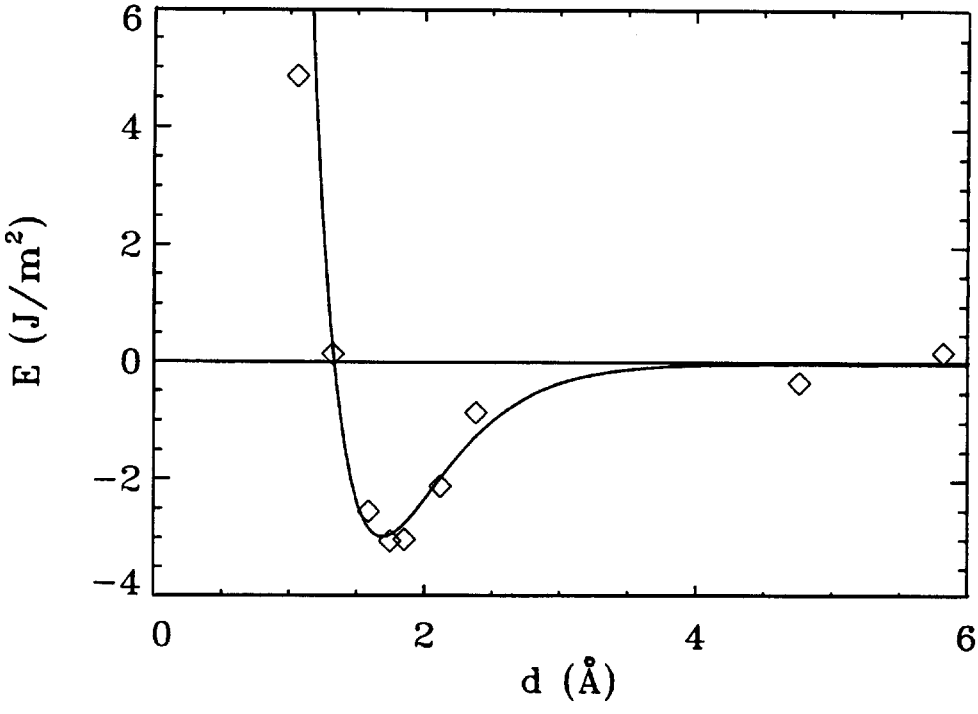

Figure 10. The unrelaxed adhesive energy of α-Al_2O_3(0001)/Cu (111) system as the function of the interfacial separation d. Computed points are shown as squares and the curve is a fit of these points to the universal binding energy relation [23].

[9] have indicated that the epitaxial Cu(111) layer on Al_2O_3(0001) is incoherent, i.e., it does not distort into registry as we have assumed to make the computation tractable. This presumably means that the misfit dislocation formation energy is greater than the increase in W_{ad} due to coherence. That coherence can increase W_{ad} was shown [26] theoretically some time ago, and this increase is in fact the driving force for misfit dislocation formation. It is not possible for us to compute the size of this effect at this time.

4. Summary

We have carried out a self-consistent, first-principles computation of the adhesive energetics for Cu/Al_2O_3. The method was first tested against the results of experiment and other calculations for Cu(111) and Al_2O_3(0001) surfaces, and good agreement was obtained. Recent TEM results [9] for MBE-grown Cu(111) on Al_2O_3(0001) helped us to establish the epitaxial geometry. The Al_2O_3(0001) substrate was taken to be Al terminated at all interfacial separations because the Al oxide formation energy is an order of magnitude larger than the Cu oxide formation energy, and because the Al-terminated Al_2O_3(0001) surface energy is almost a factor of 2 smaller than the O-terminated value. It was found that the Al_2O_3(0001) relaxation lowered the work of adhesion W_{ad} from 2.9 J/m^2 to 0.9 J/m^2. Thus we see that relaxation effects can have a large effect on W_{ad}. Our computed W_{ad} is larger than experimental values as expected, but the agreement is nevertheless reasonably good.

There are several indications of a significant metallic/covalent component to the Cu/Al_2O_3 adhesive bond. The first indication is in the electron density contours, which show some electron density concentration between Cu and O atoms. The second is the form of the W_{ad} versus interfacial separation curve. Reasonably good agreement was found with the universal binding energy relation [23], which was originally discovered for bimetallic adhesion. The third is in the computed equilibrium Cu(111)/Al_2O_3(0001) separation. The equilibrium distance between the Cu and Al

layers was found to be 1.69 Å, and the Cu and O layers are separated by 2.53 Å. These relatively large separations are suggestive of interfacial Cu atoms which have little ionic charge, since the neutral Cu atomic radius [27] is larger than the Cu^+ or Cu^{++} radii. This result is perhaps not surprising, since again the Cu oxide formation energy is substantially less than the Al oxide formation energy. However, we cannot make a quantitative conclusion about the Cu charge. In fact, when there is significant wave function overlap it is not possible to uniquely define the net charge on an atom.

While additional computations are in progress, as described below, to obtain further information on this and related interfaces, the following picture seems to be emerging. The Cu and Al atoms are competing to make bonds with the oxygen atoms. Both the Al termination layer and the first Cu layer are in contact with the first O layer (by first, we mean the layer closest to the interface). It would appear that the Al is more successful in transferring its electrons to the O atoms, as expected. This is consistent with a relatively weak W_{ad} for Cu(111)/Al_2O_3(0001). One might expect larger W_{ad} values for metals with larger oxide formation energies which are more competitive with the oxide-forming tendencies of Al. One must be mindful, however, that there is more to metal/Al_2O_3 adhesion than oxide formation. Our computations have shown that metallic/covalent contributions can be significant. The large deviations from linearity of a plot [11] of experimental W_{ad} values versus metal oxide formation energies also indicate effects beyond oxide formation.

Currently, computations are under way employing the self-consistent local orbital (SCLO) method [6, 25, 28]. The SCLO method improves upon the calculational method used here, in that electron densities and potentials are represented by a combination of plane waves and Gaussians rather than in terms of Gaussians alone as in Eqs. (7)–(8). The basis used in the SCLO method is better because the accuracy can be systematically improved by the addition of more plane waves. Variations of adhesive energetics with the metal chosen to interact with Al_2O_3 will also be computed, as will be effects of interfacial impurities.

Acknowledgments

The authors would like to thank Professor A.G. Evans and D.R. Clarke for suggesting this metal/ceramic interface and for many helpful conversations. Thanks are due also to Professor K.P. Trumble for making us aware of relevant experimental results. Support for this work is provided by the U.S. Office of Naval Research, Grant N00014-91-J4019. Access to computational facilities was provided by the San Diego Supercomputer Center and the National Energy Research Supercomputer Center.

References

1. Brian D. Flinn, Calvin S. Lo, Frank W. Zok, and Anthony G. Evans, J. Am. Ceram. Soc. **76**, 369 (1993).
2. J.F. Burgess, C.A. Neugebauer, and G. Flanagan, J. Electrochem. Soc. **122**, 688 (1972).
3. K.C. Taylor, Automobile Catalytic Converters, in *Catalysis Science and Technology*, edited by J.R. Anderson and M. Boudart (Springer-Verlag, New York, 1984), Vol. 5.
4. Kirk A. Rogers, Kevin P. Trumble, Brain J. Dalgleish, and Ivar E. Reimanis, J. Am. Ceram. Soc. **77**, 2036 (1994).
5. U. Schönberger, O.K. Andersen, and M. Methfessel, Acta Metall. Mater. **40**, Suppl., S1 (1992).
6. T. Hong, J.R. Smith, and D.J. Srolovitz, Acta Metall. Mater. **43**, 2721 (1995). Ibid., Phys. Rev. Letters **72**, 4021 (1994).
7. C. Kruse, M.W. Finnis, V.Y. Milman, M.C. Payne, A. De Vita, and M.J. Gillan, J. Am. Ceram. Soc. **77**, 431 (1994).
8. R.V. Kasowski, F.S. Ohuchi, and R.H. French, Physica B **150**, 44 (1988). These authors have carried out first-principles computations of Cu on Al_2O_3. Their results were consistent with ours in that they found the Cu bonded preferentially to the O rather than to the surface Al atoms. A detailed comparison is not possible, however, because they treated a rather different interface, i.e., a fractional monolayer of Cu on a $(10\bar{1}0)$ Al_2O_3 surface. We chose the Cu(111)/Al_2O_3 (0001) configuration because of its recent experimental [9] confirmation.
9. G. Dehm, M. Rühle, G. Ding, and R. Raj, Phil. Mag. B **71**, 1111 (1995).
10. J.E. McDonald and J.G. Eberhart, Trans. Met. Soc. AIME **233**, 512 (1965).
11. D. Chatain, L. Coudurier, and N. Eustathopoulos, Rev. Phys. Appl. **23**, 1055 (1988).
12. W.Y. Ching and Y. Xu, J. Am. Ceram. Soc. **77**, 404 (1994).
13. J.A. Appelbaum and D.R. Hamann, Solid State Commu. **27**, 881 (1978); see also P.J. Feibelman, J.A. Appelbaum, and D.R. Hamann, Phys. Rev. B **20**, 1433 (1979).
14. G.L. Zhao, T.C. Leung, B.N. Harmon, M. Keil, M. Muller, and W. Weber, Phys. Rev. B **40**, 7999 (1989); G.L. Zhao and B.N. Harmon, Phys. Rev. B, **48**, 2031 (1993); G.L. Zhao, J. Callaway, and M. Hayashibara, Phys. Rev. B, **48**, 15781 (1993).
15. J. Guo, D.E. Ellis, and D.J. Lam, Phys. Rev. B **45**, 3204 (1992).
16. J. Guo, D.E. Ellis, and D.J. Lam, Phys. Rev. B **45**, 13647 (1992).
17. M. Gautier, G. Renaud, L. Pham Van, B. Villette, M. Pollak, N. Thromat, F. Jollet, and J.P. Duraud, J. Am. Ceram. Soc. **77**, 323 (1994).
18. I. Manassidis and M.J. Gillan, J. Am. Ceram. Soc. **77**, 335 (1994).
19. P.O. Gartland, S. Berge, and B.J. Slagovold, Phys. Rev. Letters **28**, 738 (1972).
20. J.R. Smith, F.J. Arlinghaus, and J.G. Gay, Solid State Commun. **24**, 279 (1977).

21. An example of this for Nb on $Al_2O_3(0001)$ can be found in Ref. 7 and ibid., to be published.
22. Y.-N. Xu and W.Y. Ching, Phys. Rev. B **43**, 4461 (1991).
23. J.H. Rose, J. Ferrante, and J.R. Smith, Phys. Rev. Lett. **47**, 675 (1981); T. Hong, J.R. Smith, D.J. Srolovitz, J.G. Gay, and R. Richter, Phys. Rev. B **45**, 8775 (1992); A. Banerjea and J.R. Smith, Phys. Rev. B **37**, 6632 (1988).
24. R.M. Pilliar and J. Nutting, Phil. Mag. **16**, 181 (1967).
25. T. Hong, J.R. Smith, and D.J. Srolovitz, Phys. Rev. B **47**, 13, 615 (1993).
26. J. Ferrante and J.R. Smith, Surf. Sci. **38**, 77 (1973).
27. See Table 10 of *Introduction to Solid State Physics*, edited by C. Kittel, 5th edition (John Wiley & Sons, 1976).
28. J.R. Smith, J.G. Gay, and F.J. Arlinghaus, Phys. Rev. B **21**, 2201 (1980).
29. H. Wawra, Z. Metallk. **66**, 395, 492 (1975).